New Journal of Physics
The open-access journal for physics

Coupled magnetic and structural transitions in $La_{0.7}Sr_{0.3}MnO_3$ films on $SrTiO_3$

M Ziese[1,3], I Vrejoiu[2], A Setzer[1], A Lotnyk[2] and D Hesse[2]

[1] Division of Superconductivity and Magnetism, University of Leipzig, D-04103 Leipzig, Germany

[2] Max Planck Institute of Microstructure Physics, D-06120 Halle, Germany

E-mail: ziese@physik.uni-leipzig.de

New Journal of Physics **10** (2008) 063024 (8pp)

Received 24 April 2008

Published 23 June 2008

Online at http://www.njp.org/

doi:10.1088/1367-2630/10/6/063024

Abstract. The magnetic properties of three epitaxial $La_{0.7}Sr_{0.3}MnO_3$ films of thickness 5, 15 and 40 nm grown on $SrTiO_3$ (001) substrates were investigated. The structural transition of the $SrTiO_3$ substrate induces a magnetic transition in the manganite films due to magnetoelastic coupling. Below the temperature of the structural transition additional steps in the magnetization reversal characteristics appear characterized by clearly defined coercive fields. These additional coercive fields depend on the cooling history of the sample and are related to the formation of structural domains in the $La_{0.7}Sr_{0.3}MnO_3$ films induced by the substrate.

Contents

[3] Author to whom any correspondence should be addressed.

1. Introduction

Manganite films of the type $La_{0.7}Sr_{0.3}MnO_3$ (LSMO) continue to attract considerable research interest due to the strong spin–charge–phonon coupling [1]. In the field of multiferroics this leads to potential applications of manganites in heterostructures and especially to the electric control of their magnetic properties [2, 3]. It is well established that both the resistivity and magnetization of LSMO films grown on $BaTiO_3$ substrates undergo large changes at the first-order structural phase transitions of $BaTiO_3$ at 278 and 183 K [2, 4]. The influence of the structural phase transition at 105 K in $SrTiO_3$ (STO) is less well studied, although $SrTiO_3$ is a standard substrate for manganite film growth. $SrTiO_3$ undergoes a second-order phase transition at about 105 K from a high temperature cubic (Pm3m) to a low temperature tetragonal (I4/mcm) phase [5, 6]. It was shown that twinning in the substrate crystal in the tetragonal phase induces twinning in a rather thick $La_{0.67}Ca_{0.33}MnO_3$ (LCMO) film grown on it [7]. The twinning in the LCMO film was interpreted as arising from a structural transition from a tetragonal high temperature to a low temperature orthorhombic, bulk-like phase induced by the effective stress exerted by the substrate [7]. The evolution of this phase on cooling through the structural transition was not studied. In another study the influence of the cubic to rhombohedral phase transition in $LaAlO_3$ on the structural and magnetic properties of $La_{0.7}Sr_{0.3}MnO_3$ films was investigated [8]. However, since the structural transition in $LaAlO_3$ occurs at about 813 K, the influence of the transition on the ferromagnetism cannot be studied directly in this film–substrate system.

Here, the magnetic properties of three LSMO films were measured near the temperature T_S of the structural transition in the $SrTiO_3$ crystals used as substrates. This study was possible by two means: (i) the growth of very smooth LSMO films that are magnetically extraordinarily soft and (ii) by the use of high-resolution ac-susceptometry that allows for an accurate determination of the coercive fields. This study differs from the one in [7] in two ways: firstly, by the use of LSMO films instead of LCMO with LSMO being rhombohedral in the bulk and secondly, by the choice of thin films that were fully strained.

2. Experimental details

Epitaxial LSMO films were fabricated by pulsed-laser deposition using a KrF excimer laser operating at 248 nm, a ceramic LSMO target and vicinal (miscut angle 0.1°–0.2°) $SrTiO_3$ (001) single crystals as substrates [9]. Growth temperature was 600° C and oxygen partial pressure 0.3 mbar; the films were cooled down in 1 bar O_2. The films were characterized by x-ray diffractometry, atomic force microscopy (AFM) and transmission electron microscopy (TEM). In-plane lattice constants were determined from reciprocal space mapping around the (204) $SrTiO_3$ reflection, out-of-plane lattice constants were calculated from Θ–2Θ-scans. The fundamental and higher harmonic ac-susceptibility $\chi_n = \chi'_n - i\chi''_n$ was measured with a Lakeshore (ACS7000) susceptometer operating with a maximum value of the ac-field amplitude H_{ac} of 1.8 mT; the frequency was chosen at 667 Hz. Magnetic fields were applied in-plane along the [100]-direction, which is defined as the longer side of the rectangular samples. Here only data of the first χ_1 and third χ_3 harmonic susceptibility are presented. Three LSMO films of thickness 40, 15 and 5 nm as determined from deposition time and checked by TEM were investigated, see table 1.

Table 1. Parameters of the LSMO films: film thickness d, Curie temperature T_C, saturation magnetization M_S, in-plane lattice constant a and out-of-plane lattice constant c.

Sample	d (nm)	T_C (K)	$\mu_0 M_S$ (T)	a (nm)	c (nm)
LS40	40	334	0.55	0.390	0.385
LS15	15	330	0.56	–	0.385
LS05	5	295	0.52	–	–

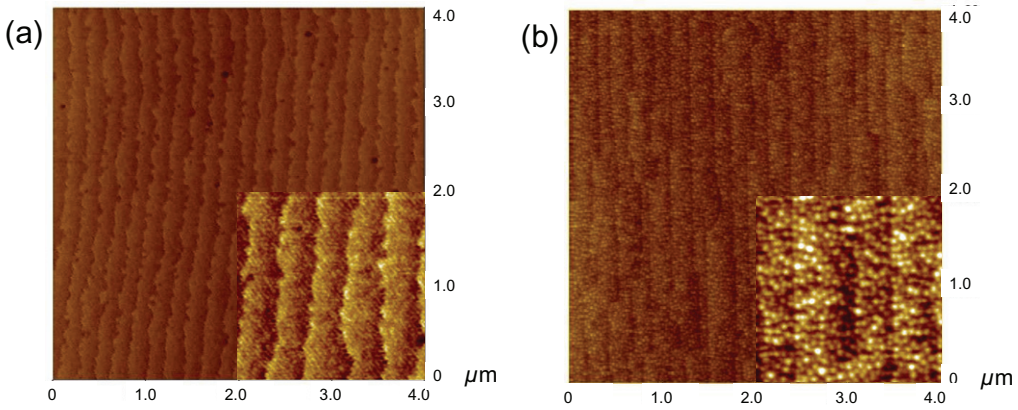

Figure 1. AFM images of the (a) 15 nm thick LSMO film LS15 and (b) 40 nm thick sample LS40. The insets show a magnification by a linear scale factor of two of central $1 \times 1\ \mu m^2$ large areas of the main image.

3. Results and discussion

X-ray diffractometry was used to study the strain state of the samples. Reciprocal space mapping around the (204) $SrTiO_3$ reflection of sample LS40 clearly showed that this sample was strained with in-plane lattice constants identical to that of the STO substrate, see table 1 [10]. Θ–2Θ-scans of samples LS40 and LS15 yielded out-of-plane lattice constants of about $c = 0.385$ nm; for the in-plane lattice parameter of LS15 and the lattice constants of LS05 no data could be obtained due to the weak x-ray scattering intensity. Since the c/a ratio of films under tensile strain decreases with decreasing thickness [10], the lattice parameters obtained on LS40 assure that $c/a < 0.987$ for the three samples, which thus show tetragonal symmetry induced by the substrate.

Figure 1 shows AFM images of $4 \times 4\ \mu m^2$ regions of samples LS15 and LS40. In the case of sample LS15, clear terraces with a width of about 200 nm and a height of one unit cell can be seen (step-flow growth regime) similar to the results on the growth of $PbZr_{0.2}Ti_{0.8}O_3$ films [9]. The film was very smooth with a root-mean-square (rms) roughness below 0.2 nm. Sample LS40 still showed indications of step-flow growth, see figure 1(b), but the structure is more grainy with the nucleation of islands being visible. The rms roughness of this film was slightly increased to 0.26 nm. All films were continuous; see [11] for further details on film preparation.

A standard magnetic characterization was performed by SQUID magnetometry with the values of the Curie temperature T_C and the saturation magnetization M_S determined from the

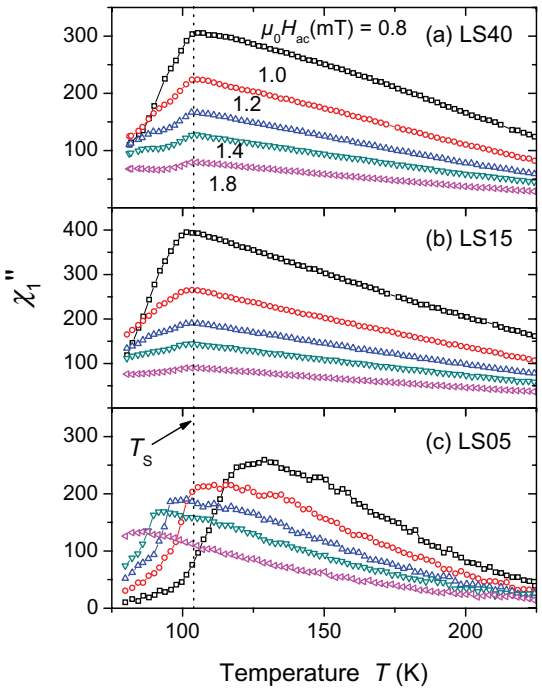

Figure 2. Loss component χ''_1 of the LSMO films of thickness (a) 40 nm, (b) 15 nm and (c) 5 nm. T_S marks the temperature of the structural transition of the $SrTiO_3$ substrate.

field-cooled magnetization in a field of 0.1 T. Within the experimental error the saturation magnetization is independent of film thickness, whereas the Curie temperature decreases significantly, see table 1.

The loss component χ''_1 of the films is shown in figure 2 as a function of temperature for ac-field amplitudes between 0.8 and 1.8 mT. The striking feature in these data is the presence of a magnetic transition independent of the ac-field amplitude in samples LS40 and LS15 at about 104 K. This appears only in the susceptibility measured with ac-field amplitudes larger than the coercive field and indicates a change in the domain-wall mobility at this temperature. Since this is very close to the literature value for the structural transition temperature T_S in $SrTiO_3$ [6], it is natural to relate the change in the domain-wall mobility to the appearance of structural domains in the LSMO films induced by the substrate deformation. Indeed twinning was observed in $La_{0.67}Ca_{0.33}MnO_3$ films on $SrTiO_3$ below 105 K [7]. The situation in the thinnest film LS05 is different with the maximum in χ''_1 shifting to lower temperatures with increasing H_{ac}. This indicates that another coercivity mechanism is active in this film.

In order to elucidate the magnetoelastic transition at T_S in more detail, measurements of χ_1 and χ_3 as a function of the ac-field amplitude H_{ac} were performed in the temperature region near T_S. Figure 3 shows the (a) real and (b) imaginary components of χ_3 for sample LS05. On cooling through T_S the form of the susceptibility curves changes drastically becoming much broader and developing a clear triple transition. Similar broadening and splitting of the transition is also seen for the other samples. This is interpreted as arising from an inhomogeneous sample state consisting of magnetic regions with different coercive fields. The inflection points in χ''_3, as indicated by the arrows in figure 3(b) can be used to determine the coercive fields [12] and the corresponding values for H_c are shown in figure 4 for all films. There are two main conclusions

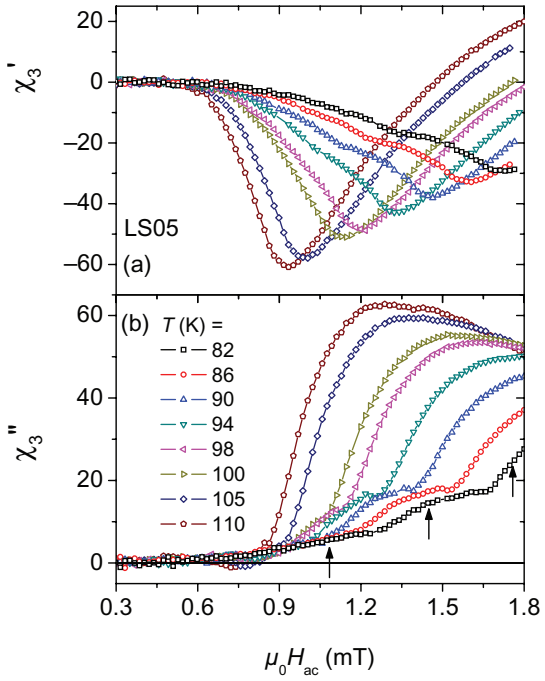

Figure 3. (a) In-phase and (b) out-of-phase components of the third harmonic ac-susceptibility of the 5 nm LSMO film for temperatures in the vicinity of T_S. The arrows indicate the three coercive fields at 82 K.

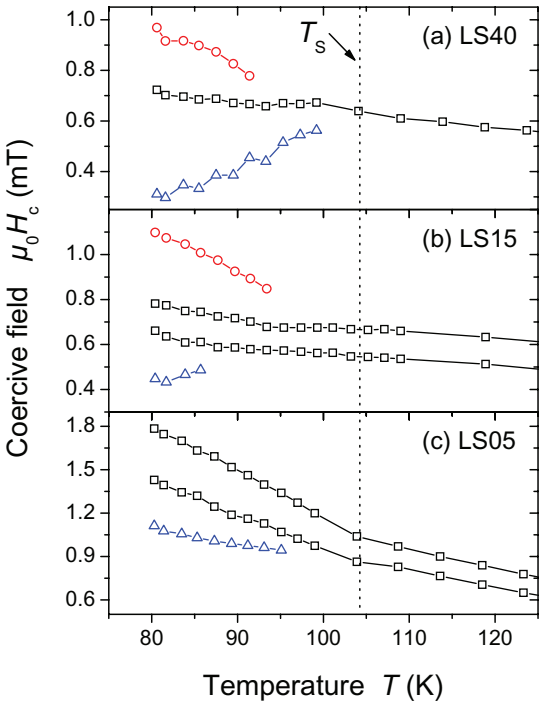

Figure 4. Coercive fields of the LSMO films of thickness (a) 40 nm, (b) 15 nm and (c) 5 nm as a function of temperature.

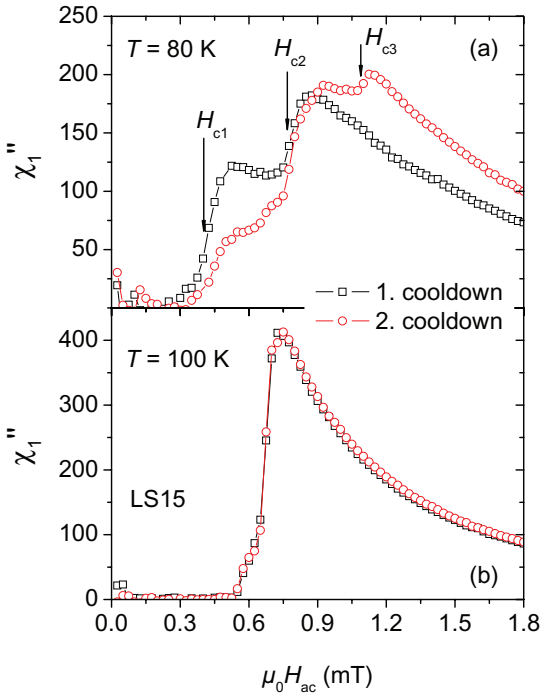

Figure 5. Loss component χ''_1 of the 15 nm thick LSMO film at (a) 80 K and (b) 100 K. The data were measured in two consecutive runs after cooling the sample from 320 to 80 K.

from this analysis: (i) below T_S additional coercive fields appear with a lower and an upper coercive field branch emerging (where the upper one cannot be detected in sample LS05 due to limitations on the maximum ac-field amplitude), (ii) for the thinner films already above T_S two coercive fields are seen (for sample LS05 above T_S there is a tiny shoulder to the main transition barely observable in figure 3(b)). Moreover, the temperature dependence of H_c is considerably stronger for sample LS05 which also points towards an additional coercivity mechanism being active in this film. On general grounds one might expect that the behaviour of the sample LS05 differs from that of the thicker films, since it is close to the orbitally ordered phase of thin LSMO films that appears below a critical thickness of about 3–4 nm [13, 14].

Figure 5 shows the loss component χ''_1 of sample LS15 at (a) 80 K and (b) 100 K after two subsequent cooldowns from 320 K. Whereas the curves at 100 K are well reproducible, at 80 K a clear dependence on the history of the sample is seen. This is interpreted as arising from the different twin-domain structures formed in the $SrTiO_3$ crystal in different cooldowns.

The high structural quality of the LSMO films is reflected in their low coercive fields. The evolution of the coercive field with temperature and film thickness suggests that both the formation of structural domains below the structural transition of the substrate as well as the microstructure of the films influence domain-wall mobility and/or magnetic domain nucleation. The thinner films LS05 and LS15 both show two coercive field branches in the complete temperature regime. Since these films show clear step-flow growth and since it is known that step edges introduce an anisotropic domain-wall mobility [15], it is tempting to relate these two coercive field branches to the influence of the step-edge pattern. This has not been further studied in detail in these films, since the main focus of the investigation was on the effects of the

structural transition on the magnetic properties. Moreover, the detailed three-dimensional strain states of the films might further influence the coercivity [16]. Sample LS05 shows a considerable temperature dependence of the coercive field and a clear break in slope of the main coercivity branches at the structural transition, see figure 4(c). This is interpreted as a coupling between the structural distortion and other coercivity mechanisms.

The main effect of the structural distortion of the STO substrate on the magnetic properties of the LSMO films is the appearance of two additional coercivity branches below T_S, see figure 4. In magneto-optical studies [7] of $La_{0.67}Ca_{0.33}MnO_3$ films on $SrTiO_3$ twinning of the LCMO films was observed in the magnetic contrast with the LCMO twin domains lying under 45° to the STO structural domains. This was interpreted as a transition of the LCMO film to an orthorhombic, bulk-like phase below T_S [7]. This interpretation does not apply here, since LSMO is not orthorhombic in the bulk and since the films are fully strained and therefore clamped to the substrate.

Here, we propose a different interpretation. It is well known that the manganite films under tensile film–substrate stress develop a magnetic easy-plane anisotropy within the film plane, whereas the compressive stress leads to a magnetic easy direction along the surface normal [10, 17]. This suggests that an elongation of the pseudo-cubic manganite cell leads to a softening of the magnetic anisotropy along that direction and vice versa for a contraction. It has further been shown that the STO crystals develop crystallographic microdomains below T_S with either the *c*-axis or the *a*-axis along the surface normal [6]. The *a*-axis domains will certainly be twinned as observed in [7]. There are thus three independent directions for the substrate *c*-axis, i.e. parallel to the substrate normal, perpendicular to the substrate normal parallel to the ac-field H_{ac} and perpendicular to both the substrate normal and ac-field.

In samples LS40 and LS15, one coercive field branch is unaffected by the structural transformation, whereas the other two are either magnetically softer or harder. The formation of these coercivity branches might now be directly related to the formation of the three differently oriented crystallographic domains. In the first, the *c*-axis of the tetragonal STO structure is oriented along the substrate normal, not significantly affecting the coercive field, whereas the magnetically softer and harder coercivity branches correspond to crystallographic domains with the STO *c*-axis in-plane either parallel or perpendicular to the ac-field direction.

4. Conclusions

In summary, the changes in the magnetic properties of LSMO films induced by the structural transition of the $SrTiO_3$ substrates were studied. The formation of structural domains in the LSMO films induced by the substrate leads to a gradual splitting of the coercive field into three branches corresponding to the three STO *c*-axis orientations inducing these domains with respect to the magnetic field.

Acknowledgments

This work was supported by the DFG within the Collaborative Research Center (SFB 762) ‘Functionality of Oxide Interfaces’. We thank B I Birajdar for the TEM measurements.

References

[1] Coey J M D, Viret M and von Molnár S 1999 *Adv. Phys.* **48** 167
[2] Eerenstein W, Wiora M, Pietro J L, Scott J F and Mathur N D 2007 *Nat. Mater.* **6** 348
[3] Thiele C, Dörr K, Bilani O, Rödel J and Schultz L 2007 *Phys. Rev.* B **75** 054408
[4] Lee M K, Nath T K, Eom C B, Smoak M C and Tsui F 2000 *Appl. Phys. Lett.* **77** 3547
[5] Shirane G and Yamada Y 1969 *Phys. Rev.* **177** 858
[6] Cao L, Sozontov E and Zegenhagen J 2000 *Phys. Status Solidi* a **181** 387
[7] Vlasko-Vlasov V K, Lin Y K, Miller D J, Welp U, Crabtree G W and Nikitenko V I 2000 *Phys. Rev. Lett.* **84** 2239
[8] Lehmann A G, Sanna C, Lampis N, Congiu F, Concas G, Maritato L, Aruta C and Petrov A Y 2007 *Eur. Phys. J.* B **55** 337
[9] Vrejoiu I, Le Rhun G, Pintilie L, Hesse D, Alexe M and Gösele U 2006 *Adv. Mater.* **18** 1657
[10] Maurice J L, Pailloux F, Bartheélémy A, Durand O, Imhoff D, Lyonnet R, Rocher A and Contour J P 2003 *Phil. Mag.* **83** 3201
[11] Vrejoiu I, Ziese M, Setzer A, Esquinazi P D, Birajdar B I, Lotnyk A, Alexe M and Hesse D 2008 *Appl. Phys. Lett.* **92** 152506
[12] Prüfer S and Ziese M 2008 *Phys. Status Solidi* b at press
[13] Konishi Y, Fang Z, Izumi M, Manako T, Kasai M, Kuwahara H, Kawasaki M, Terakura K and Tokura Y 1999 *J. Phys. Soc. Japan* **68** 3790
[14] Hong X, Posadas A and Ahn C H 2005 *Appl. Phys. Lett.* **86** 142501
[15] Haibach P, Huth M and Adrian H 2000 *Phys. Rev. Lett.* **84** 1312
[16] Nath T K, Rao R A, Lavric D, Eom C B, Wu L and Tsui F 1999 *Appl. Phys. Lett.* **74** 1615
[17] O'Donnell J, Rzchowski M S, Eckstein J N and Bozovic I 1998 *Appl. Phys. Lett.* **72** 1775